ISBN: 978-3-95450-247-9 ISSN: 2673-5490 doi: 10.18429/JACoW-IPAC2024-THPG04

RF AND MULTIPACTOR ANALYSIS FOR THE CARIE RF PHOTOINJECTOR WITH A PHOTOCATHODE INSERT *

H. Xu†, A. Alexander, P. M. Anisimov, W. C. Barkley, G. R. Bustos, T. P. Grumstrup, S. Rocha, E. I. Simakov, Los Alamos National Laboratory, Los Alamos, NM, USA
G. E. Lawler, J. B. Rosenzweig, UCLA, Los Angeles, CA, USA

Abstract

At Los Alamos National Laboratory, we developed a 1.6-cell C-band RF photoinjector for the Cathodes And Radiofrequency Interactions in Extremes (CARIE) project. The injector will be used to study the behavior of advanced photocathode materials under very high RF gradients. The photocathodes will be prepared with an INFN-style photocathode plug, compatible with the plugs used by other institutions. This presentation will report the RF design of the photoinjector with distributed coupling and RF field symmetrization. Beam physics simulations show that symmetrized RF fields in the vicinity of the beam axis are essential for minimizing the normalized emittances for a 250-pC electron bunch. We also analyze the challenges related to the photocathode insertion and reducing the peak electric fields, multipactor suppression, and resonant frequency tuning by fine adjustment of the plug position.

INTRODUCTION

Radiofrequency (RF) photoinjectors find uses in many applications. When operating with a strong field on the photocathode surface, RF photoinjectors produce bunches with high charge and reduced emittance. High-brightness electron bunches benefit applications such as ultrafast electron diffraction, inverse Compton scattering light source, and X-ray free electron laser [1, 2].

At Los Alamos National Laboratory (LANL), we study a 1.6-cell RF photoinjector at *C*-band (5.712 GHz), aiming at producing 250-pC electron bunches with a normalized emittance around 100 nm rad, at a photocathode electric field of 240 MV/m [3]. The original concept of operating a high-gradient, 1.6-cell RF photoinjector at a cryogenic temperature was first put forward by UCLA [4]. The initial 1.6-cell RF photoinjector cavity design, with distributed RF coupling, was completed at SLAC and UCLA [4, 5].

In 2022, LANL designed the RF photoinjector cavity for the initial high power test at 5.712 GHz. The initial version of the cavity did not use an aperture on the planar end of the cathode cell, aiming at understanding the RF design, especially the tuning procedure, and at investigating the high-gradient performance of the cavity [6]. In 2024, LANL completed the design of the 1.6-cell photoinjector RF cavity that accommodates the insert of an INFN-style photocathode plug, which is discussed in this paper. The geometry design of the photocathode plug insert into the cavity referred to the design of the *S*-band Pegasus photoinjector at UCLA [2], with new design features addressing new challenges posed by high-gradient operations at *C*-band.

DESIGN OVERVIEW

An illustration of the LANL *C*-band photoinjector cavity design with photocathode plug insert is provided in Fig. 1. The photocathode plug is a modified version of the INFN-style plug. The input RF power enters the cavity through the standard WR187 waveguide port. The taper waveguide connecting the WR187 port to the RF distribution waveguides is bent towards the upstream of the beamline, with the purpose of preventing the WR187 RF flange from interfering with the emittance-compensation solenoid to be installed in the downstream. A molybdenum photocathode plug is inserted into the cathode cell. On the horizontal plane, there are two laser ports pointing at the center of the photocathode plug front flat face. One port is for the incident laser, and the other one, on the opposite side, is for the reflected laser.

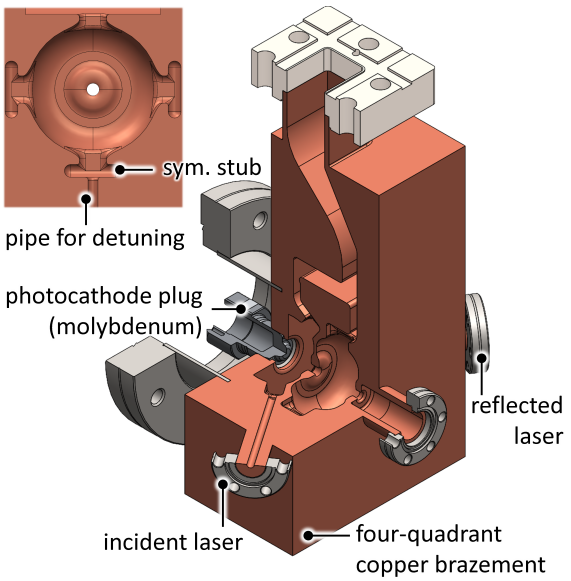

Figure 1: 3D illustration of the LANL *C*-band photoinjector cavity design with photocathode plug insert. On the top-left, a transverse cross section view is provided for the full cell of the cavity.

In Fig. 1, at top-left, a transverse cross section of the full cell is shown. The RF power is coupled into the full cell at the top, through the coupling slot. In the opposite and perpendicular directions, there are three symmetry stubs,

* Work supported by U.S. Department of Energy through the Laboratory Directed Research and Development program of Los Alamos National Laboratory, under project number 20230011DR.
† haoranxu@lanl.gov

ISBN: 978-3-95450-247-9 ISSN: 2673-5490 doi: 10.18429/JACoW-IPAC2024-THPG04

designed for the purpose of symmetrizing the perturbation to the RF fields inside the cell, introduced by the RF coupling port. The symmetry stubs are also designed for the cathode cell. At the bottom of the full cell, there is a pipe for the insertion of a detuning rod, to be operated by a linear motion feedthrough. The detuning rod is used to detune the full cell, when we would like to work on the RF tuning of the cathode cell exclusively, without the interference from the full cell. Due to the symmetry stubs and the laser pipes, the copper body of the cavity has to be fabricated by brazing four copper quadrants together.

PLUG INSERT AND MULTIPACTOR

The geometry of the molybdenum photocathode plug inserted into the cathode cell is illustrated in Fig. 2. The photocathode plug is pushed into the cathode cell. The longitudinal position of the plug is constrained by a circular knife edge, which is brazed onto the copper body of the cavity. The tip of the plug is formed by a trapezoidal step, and the photocathode film is deposited on the flat face of the tip of the plug. The edge of the step is blended for reducing the electric field enhancement.

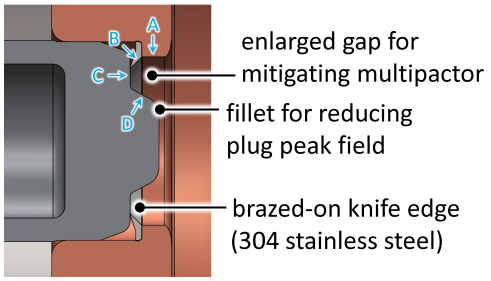

Figure 2: The designed geometry of the molybdenum photocathode plug inserted into the cathode cell. Annotations "A" to "D" are used to describe the multipactor in this region, and they denote: the copper aperture cylindrical face, the knife edge face, the plug flat face surrounding the plug-tip step, and the plug-tip side-slope face, respectively.

The cathode cell will be tuned with a photocathode plug pushed tightly against the knife edge, which provides sufficient RF sealing. In this process, the knife edge will deform elastically. During the photoinjector operation, when we replace the photocathode plugs, we plan to vary the force for pushing the plug, in order to compensate for the machining error among the different plugs, so that the correct RF tuning can be recovered in the cathode cell. This design was inspired by the Pegasus gun operation experience.

The trapezoidal plug tip and the cylindrical copper aperture form a coaxial geometry, with a large gap in between, as shown in Fig. 2. This design is for the purpose of mitigating the electron multipactor, which we studied using the CST Particle-In-Cell Solver [7]. There are two multipactor modes in this region, where the faces related to the multipactor discussion are denoted in Fig. 2, with "A" to "D." Two-point multipactor between face A and D happens at a relatively lower field level, when the cathode-center electric field is around 5 MV/m. Single-point multipactor happens on the faces B and C when the fields are stronger; the single-point multipactor is cutoff when the cathode-center electric field reaches 28 MV/m, which corresponds to an accelerating gradient of 16 MV/m in the full cell. When the cathode-center electric field is higher than 28 MV/m, secondary electrons are quickly flushed out by the stronger electric field in the region, which allows the cavity to be multipactor-free. When the photoinjector is operating with a much higher cathode-center electric field, e. g., around 100 MV/m, upon the input of the RF pulse, the cathode-center field will rise so fast that there is very limited time for the multipactor to build up a cloud of secondary electrons. This operation strategy is sometimes referred to as the "burn-through" of a multipactor barrier.

When the concentric gap between the plug tip and the copper aperture is increased, the multipactor cut-off field level is reduced, which is beneficial. However, there is a certain upper limit on the gap size, because enough space has to be reserved for the plug tip. If the diameter of the tip of the plug is too small, the radial distribution uniformity of the electric field magnitude on the flat face of the plug tip will be compromised, which, in turn, will reduce the quality of the electron bunches generated.

RF SIMULATION RESULTS

We used the CST High Frequency Solver to tune the RF photoinjector cavity to operate at 5.712 GHz with critical coupling at room temperature. The computed Smith chart plot is shown in Fig. 3, where the $S11$ coefficient is calculated at the input WR187 waveguide port. At 5.712 GHz, the power reflection was predicted to be less than −40 dB. When calculated individually, the cathode cell, together with the molybdenum photocathode plug and the 304 stainless steel knife edge, had an unloaded quality factor of 9564. The unloaded quality factor of the full cell alone was 13398. The unloaded quality factor of the entire cavity was calculated to be 11571.

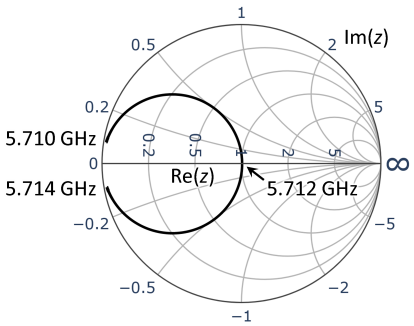

Figure 3: $S11$ calculated at the input WR187 port to the cavity, plotted in an impedance Smith chart format.

The RF power is distributed in such a way that the peak copper-surface electric fields in the two cells are equal, which resulted in the on-axis electric field magnitude distribution

ISBN: 978-3-95450-247-9 ISSN: 2673-5490 doi: 10.18429/JACoW-IPAC2024-THPG04

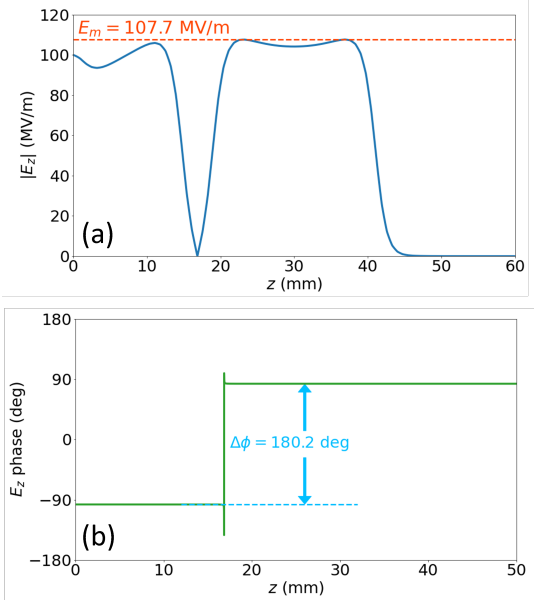

Figure 4: (a) The magnitude and (b) the RF phase distribution of the on-axis electric field.

presented in Fig. 4(a), where the peak field value is denoted as E_m. Figure 4(b) shows that the RF phase difference between the two cells is 180 degrees, indicating operation in a π-mode. In the cathode cell, the on-axis electric field profile indicates a stronger higher-order spatial harmonic content, when compared with the full cell.

In Fig. 5, the contour plots of the longitudinal RF electric field component and of the magnetic field magnitude are shown, when the photocathode plug tip center electric field

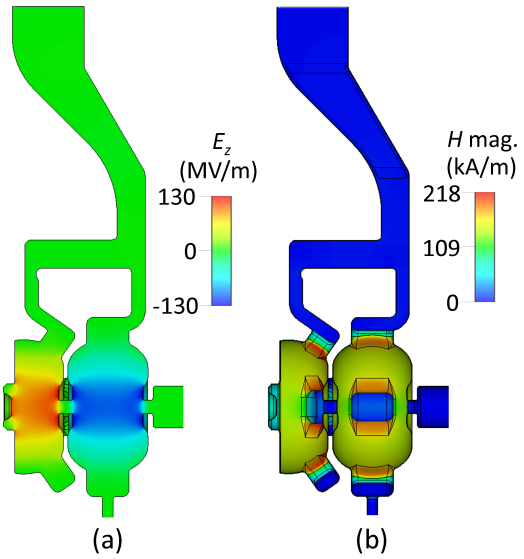

Figure 5: Contour plot of (a) the longitudinal electric field component and (b) the magnetic field magnitude in the photoinjector cavity, when the photocathode plug tip center electric field magnitude is 100 MV/m.

is 100 MV/m. The peak electric field location in the cavity is on the surface of the re-entrant features in the two cells. The peak magnetic field location in the cavity is at the coupling slot and the symmetry stubs of the cathode cell. When the cavity operates with 100-MV/m and 240-MV/m electric fields at the center of the photocathode plug, the input RF power levels of 1.8 and 10.4 MW, respectively, are required.

CONCLUSION

A 1.6-cell *C*-band radiofrequency (RF) photoinjector cavity was designed at Los Alamos National Laboratory (LANL). The cavity allows using a photocathode plug insert. The plug insert geometry was optimized towards mitigating the electron multipactor phenomenon while preserving the uniformity of the electric field on the flat surface of the tip of the plug. The specially developed approach is introduced for tuning the cathode cell. In each cell, three symmetry stubs are used to symmetrize the field perturbation induced by the coupling slot.

RF simulations showed that the designed cavity operates with a π-mode, at critical coupling at 5.712 GHz. The peak electric field in the two cells was designed to be equal. The RF design met the photoinjector operating requirements. Currently, we are working on the mechanical design of this photoinjector cavity. We will then fabricate the cavity and test it at LANL.

REFERENCES

[1] J. B. Rosenzweig *et al.*, "A high-flux compact X-ray free-electron laser for next-generation chip metrology needs," *Instruments*, vol. 8, no. 1, p. 19, Mar. 2024. doi:10.3390/instruments8010019

[2] P. Musumeci *et al.*, "Relativistic electron diffraction at the UCLA Pegasus photoinjector laboratory," *Ultramicroscopy*, vol. 108, no. 11, pp. 1450–1453, Oct. 2008. doi:10.1016/j.ultramic.2008.03.011

[3] P. M. Anisimov *et al.*, "Multi-objective genetic optimization of high charge TopGun photoinjector," presented at IPAC'24, Nashville, USA, May 2024, paper MOPS55, this conference.

[4] R. R. Robles *et al.*, "Versatile, high brightness, cryogenic photoinjector electron source," *Phys. Rev. Accel. Beams*, vol. 24, no. 6, p. 063401, Jun. 2021. doi:10.1103/PhysRevAccelBeams.24.063401

[5] G. E. Lawler *et al.*, "Design of a high-power RF breakdown test for a cryocooled *C*-band copper structure," in *Proc. NAPAC'22*, Albuquerque, USA, Aug. 2022, pp. 516–518. doi:10.18429/JACoW-NAPAC2022-TUPA81

[6] H. Xu *et al.*, "*C*-band photoinjector radiofrequency cavity design for enhanced beam generation," in *Proc. IPAC'23*, Venice, Italy, May 2023, pp. 2061–2063. doi:10.18429/JACoW-IPAC2023-TUPL139

[7] CST Studio Suite, http://www.3ds.com/products/simulia/cst-studio-suite